



Published in final edited form as:

Clin Cancer Res. 2008 February 15; 14(4): 1218–1227. doi:10.1158/1078-0432.CCR-07-1330.

Oncolytic Efficacy of Recombinant Vesicular Stomatitis Virus and Myxoma Virus in Experimental Models of Rhabdoid Tumors

Yushui Wu^{1,2}, Xueqing Lun¹, Hongyuan Zhou¹, Limei Wang¹, Beichen Sun¹, John C. Bell³, John W. Barrett⁴, Grant McFadden⁵, Jaclyn A. Biegel⁶, Donna L. Senger¹, and Peter A. Forsyth¹

¹Departments of Oncology, Clinical Neurosciences, and Biochemistry and Molecular Biology, University of Calgary, the Tom Baker Cancer Centre, and the Clark H. Smith Brain Tumour Research Centre, Calgary, Alberta, Canada

²Medical Research Center, Fuzhou General Hospital, Fuzhou, China

³Ottawa Regional Cancer Centre Research Laboratories, Ottawa, Ontario, Canada

⁴BioTherapeutics Research Group, Robarts Research Institute and Department of Microbiology and Immunology, University of Western Ontario, London, Ontario, Canada

⁵Department of Molecular Genetics and Microbiology, University of Florida, Gainesville, Florida

⁶Division of Human Genetics, Department of Pediatrics, The Children's Hospital of Philadelphia and the University of Pennsylvania School of Medicine, Philadelphia, Pennsylvania

Abstract

Purpose—Rhabdoid tumors are highly aggressive pediatric tumors that are usually refractory to available treatments. The purpose of this study was to evaluate the therapeutic potential of two oncolytic viruses, myxoma virus (MV) and an attenuated vesicular stomatitis virus (VSV^{ΔM51}), in experimental models of human rhabdoid tumor.

Experimental Design—Four human rhabdoid tumor cell lines were cultured *in vitro* and treated with live or inactivated control virus. Cytopathic effect, viral gene expression, infectious viral titers, and cell viability were examined at various time points after infection. To study viral oncolysis *in vivo*, human rhabdoid tumor cells were implanted s.c. in the hind flank or intracranially in CD-1 nude mice and treated with intratumoral (i.t.) or i.v. injections of live or UV-inactivated virus. Viral distribution and effects on tumor size and survival were assessed.

Results—All rhabdoid tumor cell lines tested *in vitro* were susceptible to productive lethal infections by MV and VSV^{ΔM51}. I.t. injection of live MV or VSV^{ΔM51} dramatically reduced the size of s.c. rhabdoid tumor xenografts compared with control animals. I.v. administration of VSV^{ΔM51} or i.t. injection of MV prolonged the median survival of mice with brain xenografts compared with controls (VSV^{ΔM51}: 25 days versus 21 days, log-rank test, $P = 0.0036$; MV: median survival not reached versus 21 days, log-rank test, $P = 0.0007$). Most of the MV-treated animals (4 of 6; 66.7%) were alive and apparently “cured” when the experiment was arbitrarily ended (>180 days).

© 2008 American Association for Cancer Research.

Requests for reprints: Peter A. Forsyth, Clark H. Smith Brain Tumour Research Centre, Southern Alberta Cancer Research Institute, Room 2AA19 Health Research Innovation Centre, 3330 Hospital Drive NW, Calgary, Alberta, Canada T2N 4N1. Phone: 403-210-3934; Fax: 403-210-8135; pforsyth@ucalgary.ca.

Y.Wu and X. Lun contributed equally to this work and share first authorship. D.L. Senger and P.A. Forsyth share senior authorship.

Note: Supplementary data for this article are available at Clinical Cancer Research Online (<http://clincancerres.aacrjournals.org/>).

Conclusions—These results suggest that VSV^{ΔM51} and MV could be novel effective therapies against human rhabdoid tumor.

Rhabdoid tumors are rare but highly aggressive neoplasms that occur predominantly in infants and children who are <2 years old. Although originally described as a tumor of the kidney composed partly or entirely of rhabdoid cells (1), rhabdoid tumor can develop in most soft tissues, including the liver, lung, and thymus, as well as the brain and spinal cord (2,3). Rhabdoid tumors arising in the kidney or in extrarenal sites outside of the central nervous system are generally called malignant rhabdoid tumors. Rhabdoid tumor in the central nervous system, called atypical teratoid/rhabdoid tumor, was first recognized in 1987 (4), and is usually composed of rhabdoid cells juxtaposed with areas of primitive neuroepithelial cells, mesenchymal tissue, and/or epithelial tissue. The prognosis of patients with atypical teratoid/rhabdoid tumor is very poor, as these tumors progress rapidly and are often refractory to available treatments (2). Current estimates suggest a 2-year survival rate of only 15% for children diagnosed with atypical teratoid/rhabdoid tumor (5) and new treatments are urgently needed.

The cellular origin of rhabdoid tumor is not known. Given the ability of rhabdoid tumor to arise in multiple tissue sites and to differentiate along neural, epithelial, and mesenchymal lines, it has been proposed that the cell of origin is a primitive progenitor cell that may be derived from the neural crest (3). Despite the variability observed in tumor location and histology, most rhabdoid tumors share a similar genetic origin and are characterized by the presence of mutations or deletions of the *hSNF5/INI1* gene on chromosome band 22q11.2 (5–7). Approximately 70% of primary tumors carry mutations and/or deletions in both copies of the *hSNF5/INI1* gene, whereas an additional 20% to 25% of tumors have reduced expression at the RNA or protein level, indicating that loss-of-function of the INI1 protein is a central event in the development of malignant rhabdoid tumor (5).

Although the precise mechanisms through which loss of INI1 leads to tumorigenesis are unclear, several *in vitro* and *in vivo* studies suggest that loss of INI1 perturbs key cell cycle control and DNA repair mechanisms such as the p16INK4a-Rb-E2F and p53 pathways (5,8,9). INI1 is an invariant protein in the SWI/SNF chromatin-remodeling complex, which regulates cellular gene expression programs by facilitating transcriptional activation and repression (10). The SWI/SNF complex is also implicated in the regulation of IFN signaling pathways that are important in the control of cell growth/apoptosis and in antiviral responses. In response to viral infection, normal cells rapidly up-regulate the expression and secretion of type 1 IFNs, which bind to cell surface receptors on both infected and neighboring uninfected cells and initiate signals that induce the expression of multiple genes with antiviral functions. Many tumor cells are known to have diminished responsiveness to IFN (11), which allows them to escape IFN-mediated growth control pathways, but also weakens their resistance to viral infection. Recently, knockdown of INI1 expression using RNA interference in mammalian cells was shown to block the cellular antiviral responses by inhibiting the expression of IFN- and virus-inducible genes (12). If loss of INI1 impairs the innate antiviral response in rhabdoid tumor, these tumors might be particularly susceptible to treatment with oncolytic viruses.

Oncolytic viruses are attractive new tools for the treatment of cancer due to their ability to infect and kill tumor cells, while sparing normal cells (for review, see ref. 11). Oncolytic viruses specifically target cancer cells because many of the same genetic defects that promote tumorigenesis also compromise the antiviral defenses of the cell. A number of different viruses, including both naturally occurring and genetically engineered strains, have shown promising results in preclinical testing (13–19) and in clinical trials (20,21).

Oncolytic viruses used for human cancer therapy should ideally meet several criteria (11,22). Such viruses should efficiently replicate within cancer cells and spread within tumors, but be restricted from infecting normal cells, and they should be able to be effectively delivered to multiple sites to treat invasive cells and disseminated metastases. Other desirable properties of oncolytic viruses include the ability to genetically engineer the virus to improve its safety and efficacy, as well as a nonpathogenic profile in humans, so that it is safe for patients, their families, and the community. Both myxoma virus (MV) and vesicular stomatitis virus (VSV Δ M51), an attenuated strain of vesicular stomatitis virus, fulfill many of these criteria.

MV is a rabbit-specific poxvirus that causes the lethal disease myxomatosis in the European rabbit (23). Like other poxviruses, its large double-stranded DNA genome is amenable to the potential insertion of large, therapeutically relevant, eukaryotic genes (23,24) and it is nonpathogenic in all other vertebrate species tested, including humans (25,26). Despite this narrow species selectivity, MV has oncolytic activity against human tumor cells *in vitro* and *in vivo* (15,27,28).

Vesicular stomatitis virus is a negative-stranded RNA virus belonging to the Rhabdoviridae family that is capable of infecting a wide variety of cell types, although it is not known to cause any disease in humans (29). Wild-type VSV is a potent oncolytic virus, but it is lethal when administered to animals that have not been prophylactically treated with IFN (30). The viral matrix (M) protein blocks IFN induction in cells infected with VSV, an event that is critical for successful viral replication, as IFN severely restricts VSV growth (29,31). The attenuated VSV Δ M51 strain has a single amino acid deletion of methionine-51 (M51) of the M protein, rendering it unable to block cellular IFN responses (30), thereby selectively targeting VSV Δ M51 to tumor cells with defective IFN responses (22,32). VSV Δ M51 is well tolerated when injected *i.v.*, and this method of systemic administration has the advantage of enabling the virus to target invasive multifocal tumors, including those that have widely metastasized (19,30,33,34).

In this study, we evaluated the efficacy of VSV Δ M51 (19,30) and MV (15,23) in experimental models of rhabdoid tumor. Both of these viruses have significant oncolytic activity in other brain tumor models, including glioma and medulloblastoma, which, like atypical teratoid/rhabdoid tumor, are aggressive, invasive, and difficult to treat (15,19,35). Here, we show that VSV Δ M51 and MV are effective and safe oncolytic agents against *in vitro* and *in vivo* experimental models of malignant rhabdoid tumor. The results of this study suggest that further investigation of the utility of oncolytic viruses in the treatment of malignant rhabdoid tumor is warranted.

Materials and Methods

Cell lines and animals

Rhabdoid tumor cell lines [BT-12, BT-16, STM-91-01 (36), and TM-87-16 (37)] were maintained in RPMI 1640 (Hybri-care, American Type Culture Collection) supplemented with 20% fetal bovine serum, 1% L-glutamine, and 1% insulin-transferrin-selenium (Life Technologies) at 37°C in a humidified 5% CO₂ incubator. BT-12 and BT-16 were established from brain tumors, whereas STM-91-01 and TM-87-16 were from the lung or a retroperitoneal mass, respectively. Each of the cell lines has loss of INI1 due to a homozygous mutation or deletion of the *INI1* gene. The human glioma cell line, U87, and murine fibroblast NIH 3T3 cells were purchased from the American Type Culture Collection and were cultured in DMEM/F12 medium containing 10% fetal bovine serum. Cultures were routinely tested for *Mycoplasma* contamination.

CD-1 nude mice (female, 6–8 weeks old) were purchased from Charles River Canada. The animals were housed in groups of three to five in a vivarium maintained on a 12-h light/dark schedule with a temperature of 22 ± 1 °C and a relative humidity of $50 \pm 5\%$. Food and water were available *ad libitum*. All procedures were reviewed and approved by the University of Calgary Animal Care Committee and were carried out in accordance with the Care and Use of Experimental Animals Guide issued by the Canadian Council on Animal Care.

Viruses and cell infection

VSV Δ M51, an attenuated VSV strain derived from the Indiana serotype of VSV, was propagated on Vero cells. This recombinant virus was modified by deletion of methionine 51 in the M protein and insertion of an extra cistron encoding green fluorescent protein (GFP) between the G and L sequences (30). The MV used, vMyxgfp, was derived from strain Lausanne and has a GFP cassette driven by a synthetic vaccinia virus early/late promoter inserted between open reading frames M135R and M136R of the myxoma genome (38); it was propagated on BGMK cells. Inactivated control virus [“dead” virus (DV)] was prepared by irradiating live viruses with UV light for 1 h.

For experiments examining cytopathic effect and cell viability, cells were grown to 50% to 60% confluence in 96-well plates and then infected with different doses of VSV Δ M51 [multiplicity of infection (MOI) = 0, 0.01, 0.1, or 1] or MV (MOI = 0, 1, 10, or 40) for 1 h at 37°C in 50 μ L of culture medium. Fresh medium (150 μ L) was added, and cells were cultured until the time points indicated in each experiment. Cell viability was measured 72 h post infection using the 3-(4,5-dimethylthiazol-2-yl)-5-diphenyltetrazolium bromide (MTT) assay as previously described (13). All experiments were done in triplicate. Phase-contrast and fluorescent images of cells were taken using a Carl Zeiss inverted microscope (Axiovert 200M) mounted with a Carl Zeiss digital camera (AxioCam MRc).

Viral recovery assay

Rhabdoid tumor cell lines were infected *in vitro* with 0.1 MOI of vMyxgfp or VSV Δ M51, as described above. At different time points after infection (0, 24, 48, 72, and 96 h), the cell culture plates were frozen and thawed twice to lyse cells and release viral particles. Viral titers of vMyxgfp and VSV Δ M51 in the cell lysates were determined using a standard plaque-forming assay with BGMK or L929 cells, respectively (15,19). Serial dilutions of cell lysates were cultured on confluent layers of BGMK or L929 cells, and viral titers were determined by counting fluorescent viral foci 48 h later using a Zeiss Axiovert microscope and a $\times 2.5$ low-power objective. Viral titers were calculated based on 10,000 cells.

In vivo studies in a CD-1 nude mouse model with s.c. malignant rhabdoid tumor xenografts

CD-1 nude mice received a s.c. injection of 5×10^5 STM-91-01 cells in the hind flank. When palpable tumors measuring ~ 16 mm² (length \times width) were present, MV ($n = 4$) or VSV Δ M51 ($n = 4$) was injected intratumorally [i.t.; 1×10^7 plaque-forming units (pfu)/mouse/injection] on three separate occasions at intervals of 2 days. Animals receiving i.t. injections of PBS ($n = 4$) were used as mock controls. Tumor size was measured every 3 days after virus injection for 1 month.

In vivo studies in a CD-1 nude mouse model with atypical teratoid/rhabdoid tumor brain xenografts

The stereotactic techniques used to implant atypical teratoid/rhabdoid tumor cells in the brains of CD-1 nude mice have been described previously (13). Mice were anesthetized, a burr hole was drilled through a scalp incision, and BT-16 tumor cells (2×10^5 per mouse) were inoculated into the right putamen under the guidance of a stereotactic frame (Kopf Instruments). Live or

inactivated VSV Δ M51 (5×10^8 pfu/mouse/injection) was injected i.v. via the tail vein 8, 10, and 12 days after atypical teratoid/rhabdoid tumor cell implantation. Live or inactivated MV was injected i.t. (1×10^7 pfu/mouse/injection) 8, 10, and 12 days after tumor implantation.

Mice were monitored daily and were sacrificed when they lost 20% of their body weight or had difficulty ambulating, feeding, or grooming. Tumor size was assessed 25 days after the first injection of virus. Mice were anesthetized, perfused intracardially with PBS, and then fixed with 4% paraformaldehyde. The whole brain was cut into coronal sections, and the section with the largest amount of tumor was used to measure tumor size by quantitating the tumor area and the total brain area using ImagePro software. For experiments assessing survival, animals were monitored for 180 days, at which point the experiment was terminated.

For assessment of viral replication *in vivo*, nude mice with established BT-16 brain xenografts were injected i.t. with MV (5×10^6 pfu/mouse) or VSV Δ M51 (5×10^8 pfu/mouse) 12 days after tumor implantation. On days 1, 3, 7, 14, and 21 after infection, mice were sacrificed and perfused with sterile PBS. Images of the whole brain were taken with a Leica MZ-FLIII fluorescence stereomicroscope using a standard GFP filter set. Brain tumor tissues were then stored frozen for viral culture, or embedded in OCT for H&E staining and immunohistochemistry for viral antigens.

For viral recovery assays done on brain tumor tissue, mice were perfused with PBS before euthanization and brain tumor tissue was removed under sterile conditions. The tissue was washed twice with PBS and homogenized using a Pellet Pestles Kit (VWR International) or homogenizer (Ultra-Turrax T25, Janke & Kunkel), followed by a freeze-thaw protocol to release virus from cells. Supernatants were clarified by centrifugation, diluted, and analyzed using a standard plaque-forming assay, as described above.

Immunohistochemistry for viral protein expression

Frozen sections were fixed with 4% paraformaldehyde for 20 min, followed by three washes with PBS. The sections were exposed to a rabbit polyclonal myxoma antibody, M-T7 (7,38), diluted 1:2,000 in PBS containing 2% bovine serum albumin or a rabbit polyclonal VSV antibody at a 1:3,000 dilution in PBS for 24 h at 4 °C. Biotinylated anti-rabbit IgG (Vector Laboratories) was used as a secondary antibody. Sections were then incubated with avidin conjugated to horseradish peroxidase (Vectastain ABC immunohistochemistry kit, Vector Laboratories), and staining was visualized by the addition of 3,3'-diaminobenzidine. To visualize MV and VSV antigens, sections were mounted and viewed with a Zeiss inverted microscope (Axiovert 200M) and a Carl Zeiss camera (AxioCam MRc) to obtain images.

Statistical analyses

Statistical Analysis Software (SAS Institute, Inc.) and GraphPad Prism (version 4; GraphPad Software, Inc.) were used for statistical analyses. Two-way ANOVA and the Mann-Whitney test were used to compare the tumor sizes in the s.c. and brain xenograft models, respectively. Survival curves were generated using the Kaplan-Meier method and compared using the log-rank test.

Results

VSV Δ M51 and MV productively infect and kill rhabdoid tumor cell lines *in vitro*

We evaluated the permissiveness of infection and the extent of cell killing by VSV Δ M51 and MV in four rhabdoid tumor cell lines. Two of these cell lines (BT-12 and BT-16) were derived from atypical teratoid/rhabdoid tumors. STM-91-01 cells were derived from a lung metastasis in a child with a renal malignant rhabdoid tumor (36), whereas TM-87-16 cells were isolated

from a malignant pleural effusion in a patient with a retroperitoneal mass (37). Each cell line was exposed to live or UV-inactivated-DV VSV Δ M51 (1 MOI) or MV (10 MOI), cultured for 72 h, and then examined for evidence of viral infection. As shown in Fig. 1, all of the rhabdoid tumor cell lines examined were permissive to VSV Δ M51 and MV infection, although to different degrees. Visible cytopathic effect was evident in the altered cell morphology and decreased cell numbers were present in cultures exposed to live virus, compared with the DV-treated cells (Fig. 1A and C). The expression of virally encoded GFP in all of the live virus – treated rhabdoid tumor cell lines confirmed the presence of a productive viral infection in the cells (Fig. 1A and C). None of the DV-treated cells showed any evidence of CPE or GFP expression. We have previously shown that the human glioma cell line U87 is permissive to infection with MV and VSV Δ M51, whereas the murine fibroblast cell line NIH 3T3 is resistant to infection by both viruses (15,19), and we used these cell lines as positive and negative controls. As expected, CPE and GFP expression were observed when U87 cells were exposed to live MV and VSV Δ M51, but were not observed in similarly treated NIH 3T3 cells (Fig. 1A and C).

A cell viability assay (MTT) confirmed the results from the CPE assays and quantified the extent of cell killing by MV and VSV Δ M51

All four of the malignant rhabdoid tumor cell lines were susceptible to killing by MV, and extensive cell death was observed 72 h postinfection at an MOI of 10 (Fig. 1B). Similarly, all malignant rhabdoid tumor cell lines examined were susceptible to infection and killing by VSV Δ M51, as <30% of the cells remained viable 72 h after infection with 0.1 MOI of live virus (Fig. 1D). There was no evidence of any effect on cell viability in DV-treated cells (Fig. 1B and D).

The ability of viral progeny produced during an infection to spread and infect other cells within the main tumor mass, as well as invasive and metastatic cells, is important for the therapeutic efficacy of replication-competent oncolytic viruses. Therefore, we evaluated the amount of infectious, replication-competent virus produced following infection of rhabdoid tumor cells *in vitro* with 0.1 MOI of VSV Δ M51 or MV. In all the malignant rhabdoid tumor cell lines examined, VSV Δ M51 and MV titers were substantially elevated compared with the original input viral titer as early as 24 h postinfection, with titers remaining at elevated levels for up to 96 h (Fig. 2). A similar increase in viral titer was observed in virus-treated positive control U87 cells (Fig. 2). In contrast, there was no evidence of viral propagation in the nonpermissive NIH 3T3 cells, where viral titers did not increase above the original input dose at any time point examined (Fig. 2).

VSV Δ M51 and MV have antitumor activity in a s.c. mouse model of human malignant rhabdoid tumor

Having determined that MV and VSV Δ M51 could infect and kill rhabdoid tumor cells *in vitro*, we next designed a series of experiments to determine if oncolysis by these viruses would also be observed *in vivo*. A human malignant rhabdoid tumor xenograft mouse model was created by injecting STM-91-01 cells s.c. in the hind flank of CD-1 nude mice. When the tumors had grown to ~16 mm² in size (length \times width), the mice were treated with three separate i.t. injections of live MV or VSV Δ M51 (1×10^7 pfu/injection/mouse) at intervals of 2 days. As shown in Fig. 3B, tumors injected with live MV or live VSV Δ M51 began to decrease in size 6 to 9 days after the first virus injection and continued to shrink over the 30-day time course examined. One tumor injected with MV disappeared completely, and only small residual tumors were present in the remaining MV-treated animals (Fig. 3A and B; two-way ANOVA, $P < 0.0001$). VSV Δ M51 was even more effective than MV, with the disappearance of tumors in all of the VSV Δ M51-treated mice by 30 days after virus treatment (Fig. 3A and B; two-way ANOVA, $P < 0.0001$). Tumors in mock control animals, which were injected with PBS,

continued to increase in size during the entire time course of the experiment, eventually reaching an average size of 65 mm² (Fig. 3A and B).

VSV^{ΔM51} and MV productively and selectively infect human rhabdoid tumor brain xenografts in CD-1 nude mice

In the flank model described above, STM-91-01 cells (derived from a lung metastasis of a renal tumor) were used to examine the efficacy of the oncolytic viruses at an extracranial site. To investigate the efficacy of MV and VSV^{ΔM51} against intracranial atypical teratoid/rhabdoid tumor *in vivo*, we established a mouse xenograft model of human atypical teratoid/rhabdoid tumor by implanting BT-16 atypical teratoid/rhabdoid tumor cells into the brains of CD-1 nude mice.

To assess the efficacy of intracranial BT-16 model, we used MV and VSV in the individual routes of delivery for each virus. Previously, we have shown that animals given intracranial administration of VSV^{ΔM51} will die within a few days even at very low doses, whereas systemic administration using tail vein injection is well tolerated and has oncolytic activity against human glioma brain xenografts (19). Conversely, we have shown that MV delivered intracranially is safe and well tolerated (15) but when delivered i.v. as assessed using the BT-16 intracranial rhabdoid model, is undetectable in the tumor even at time points as early as 24 and 72 h following administration (Fig. 4A). Consistent with these data, we found that i.v. administration of MV did not prolong survival of animals bearing BT-16 intracranial tumors (Fig. 4B). Therefore, to determine whether VSV^{ΔM51} and MV were able to productively infect and replicate within the brain xenograft tumors, we optimized the mode of delivery for each individual virus. Twelve days after tumor implantation, animals were given an i.t. injection of MV (1×10^7 pfu/mouse/injection) or an i.v. injection of VSV^{ΔM51} (5×10^8 pfu/mouse/injection). Animals were sacrificed at various time points after virus injection (3 animals per time point), and the expression of virally encoded GFP in the whole brain was visualized by immunofluorescence microscopy (Fig. 5A and C). At all time points examined, GFP expression was evident only in the tumor, and was not observed in other regions of the brain (Fig. 5A and C; *top 2 rows of each panel*). Viral GFP expression was observed up to 7 days after injection of VSV^{ΔM51} (Fig. 5C), but persisted at least 21 days after mice were injected with MV (Fig. 5A). Immunohistochemical staining for MV or VSV^{ΔM51} viral proteins confirmed the presence and distribution of each virus within the tumor (Fig. 5A and C, *bottom 2 rows of each panel*). To further examine the ability of the viruses to replicate *in vivo*, we isolated brain tumor tissue from animals at each time point (3 mice per time point) and did viral recovery assays to quantify the amount of infectious virus. MV titers reached maximal levels 7 to 14 days after virus treatment (Fig. 5B), whereas VSV^{ΔM51} titers peaked at 3 days postinfection (Fig. 5D). In addition, there was no evidence of infectious MV or VSV^{ΔM51} in the contralateral, nonimplanted brain hemisphere (data not shown).

VSV^{ΔM51} and MV inhibited tumor growth and prolonged survival of mice bearing atypical teratoid/rhabdoid tumor brain xenografts

As an initial assessment of the antitumor activity of the viruses in the atypical teratoid/rhabdoid tumor model, CD-1 nude mice bearing BT-16 brain xenografts were treated with live or UV-inactivated (DV) VSV^{ΔM51} (i.v., 5×10^8 pfu/mouse/injection) or MV (i.t., 1×10^7 pfu/mouse/injection) 8, 10, and 12 days after tumor implantation, and tumor size was measured 25 days after implantation. We found that all DV-treated animals had large tumors [which occupied, on average, 44% (DV, MV) and 45% (DV, VSV^{ΔM51}) in coronal sections of the brain; Fig. 6A and C]. Tumors in mice treated with i.v. VSV^{ΔM51} were significantly smaller than those in DV-treated controls (occupied on average, 35% of coronal sections of brain; Mann-Whitney, $P = 0.0068$, Fig. 6D). The largest reduction in tumor size was observed in mice injected i.t.

with MV, which was considerably more effective than i.v. VSV Δ M51 (tumors occupied, on average, 10% of coronal section of brain; Mann-Whitney, $P = 0.0003$; Fig. 6B).

We then examined the effect of virus treatment on survival. I.t. administration of live MV dramatically prolonged survival (mean time not reached) compared with the DV controls (mean, 21 days; 95% confidence interval, 19–23 days; log-rank test, $P = 0.0007$), and four of six mice treated with live MV were long-term survivors and apparently “cured” (Fig. 6E). Because only two of the live MV-treated mice died, the median survival of the live MV-treated animals was not reached (>180 days). Systemic administration of VSV Δ M51 was less effective than i.t. MV, as all of the mice treated with live VSV Δ M51 eventually died, although the median survival of the live VSV Δ M51-treated animals was significantly longer (mean, 25 days; 95% confidence interval, 23–27 days) than the DV control group (mean, 21 days; 95% confidence interval, 20–23 days; log-rank, $P = 0.0036$; Fig. 6F).

Discussion

At present, there is no standardized treatment regimen for malignant rhabdoid tumor or atypical teratoid/rhabdoid tumor and most children are treated with a combination of surgery, chemotherapy, and/or radiation (5,7). Despite aggressive multimodality treatment, the prognosis for most patients is extremely poor; in the case of atypical teratoid/rhabdoid tumor, few patients ($\leq 20\%$) survive >12 months after diagnosis (39,40). Here, we evaluated a novel therapeutic approach using two different oncolytic viruses, VSV Δ M51 and MV, and show that both of these viruses are effective oncolytic agents against *in vitro* and *in vivo* experimental models of rhabdoid tumor.

Although the molecular signaling defects in rhabdoid tumor cells that render them susceptible to infection with these oncolytic viruses are not fully understood, other work suggests that several pathways are likely to be important. Permissiveness to MV infection is closely correlated with the level of activated Akt kinase, and nonpermissive tumor cells become susceptible to MV oncolysis after expression of a constitutively active Akt mutant (28,41). Consistent with these results and previously published data (42), we found that all four tumor cell lines had higher levels of phosphorylated Akt than the nonpermissive NIH3T3 cell line (Supplementary Figure). Thus, MV could be a useful therapeutic agent in at least a subset of rhabdoid tumor. Cui et al. (12) have shown that normal functioning of INI1 in SWI/SNF complexes in HeLa cells is essential for the up-regulation of many genes in response to type I IFN. Because VSV Δ M51 replication is strongly inhibited by IFN, defective IFN signaling caused by the loss of INI1 is likely to be an important determinant of rhabdoid tumor permissiveness to VSV Δ M51. Although further work is necessary to confirm that the IFN response in rhabdoid tumor cells is similarly inhibited by the loss of INI1, inactivation of the *INI1* gene in virtually all rhabdoid tumors suggests that IFN sensitive oncolytic viruses such as VSV Δ M51 may be effective against a majority of rhabdoid tumors.

Despite a rapidly increasing number of studies examining the utility of oncolytic viruses against many cancers, there have been few comparisons of the efficacy or toxicity of multiple oncolytic viruses in a single model (19,43). Here, we have directly compared the oncolytic efficacy of MV and VSV Δ M51 *in vivo* in a s.c. flank model of malignant rhabdoid tumor using the same dose and mode of administration for both viruses. Our results show that both viruses were able to significantly shrink tumors when injected directly into the tumor mass, although VSV Δ M51 was somewhat more effective than MV. These observations are consistent with our *in vitro* results, which showed that although both viruses productively infect and kill rhabdoid tumor cells, generally the rhabdoid tumor cell lines examined were sensitive to lower doses of VSV Δ M51, and VSV Δ M51 replicated to higher titers than MV in malignant rhabdoid tumor cells that were exposed to the same initial dose of each virus. We were unable to directly compare

the efficacy of i.t. injection in the brain xenograft model used here due to the toxicity of intracerebral administration of VSV Δ M51 (19). In the brain xenograft model, i.t. injection of MV was much more effective than systemic administration of VSV Δ M51. Viral recovery assays showed that VSV Δ M51 rapidly replicated in the atypical teratoid/rhabdoid tumor xenografts *in vivo*, reaching titers higher than those observed for MV (Fig. 5B and D); however, this response was short lived and infectious VSV Δ M51 was no longer detectable in the tumor tissue after 14 days. In contrast, although MV titers increased more slowly, MV infection *in vivo* was much more persistent, with elevated titers present at least 21 days after virus treatment. This persistent infection may have allowed MV to more efficiently spread within the tumor, leading to infection and oncolysis of many more tumor cells. Other studies of oncolytic viruses have shown that insufficient viral delivery and spread is a key limitation in the treatment of brain tumors (11,30,44,45). In the future, strategies designed to improve the spread of VSV Δ M51 within the brain and within tumors might improve the efficacy of systemic VSV Δ M51 treatment. However, because MV is safe and nontoxic when injected intracerebrally (15), and was effective in the brain xenograft mouse model used here, i.t. administration of MV could be particularly advantageous in the treatment of atypical teratoid/rhabdoid tumor tumors. Systemic administration of VSV Δ M51, on the other hand, would potentially be better suited to the treatment of extracranial malignant rhabdoid tumor, particularly in situations where metastatic lesions were present.

Another consideration in selecting treatment modalities is related to the underlying genetic etiology of rhabdoid tumor. Patients with malignant rhabdoid tumor and atypical teratoid/rhabdoid tumor often have a germline mutation or deletion of the *INI1* gene that predisposes them to the development of rhabdoid tumors (5). It is not known whether the nontumor cells in these patients have impaired IFN responses, or whether there is sufficient INI1 expression from the normal allele to protect nontumor cells from viral therapy. Under these circumstances, i.t. therapy may be safer than i.v. therapy, which will also need to be considered when designing studies in patients with rhabdoid tumor.

Although this study shows that VSV Δ M51 and MV have potent oncolytic activity in several preclinical models of malignant rhabdoid tumor, both of the *in vivo* models used here are limited by the use of immunocompromised mice. In immunocompetent animals, antiviral immune responses can severely limit delivery of virus to the tumor, especially when administered i.v. (46). We have recently described a novel strategy in which virus is administered in carrier cells, which hide viral antigens during delivery and circumvent the host immune responses that normally impede viral delivery (46). Enhancement of viral oncolysis by the use of combination therapy with other drugs that sensitize tumor cells to viral infection and/or diminish antiviral immune responses may also be useful. In this regard, we have recently shown that the oncolytic activity of MV is synergistically increased when used in combination with rapamycin both *in vitro* (28) and *in vivo* in a murine brain xenograft model of medulloblastoma (47). Further evaluation of the safety and efficacy of MV and VSV Δ M51 in immunocompetent tumor models that incorporate these and other strategies is needed to determine whether oncolytic virotherapy will be useful in the treatment of malignant rhabdoid tumor.

Supplementary Material

Refer to Web version on PubMed Central for supplementary material.

Acknowledgments

We thank Laura Zajchowski for editorial assistance, and Clark H. Smith and family for their generous support.

Grant support: National Cancer Institute of Canada with funds raised by the Canadian Cancer Society (G. McFadden, P.A. Forsyth, and D.L. Senger) and a program project grant from the Terry Fox Foundation (J.C. Bell, P.A. Forsyth,

G. McFadden, and D.L. Senger); NIH grant CA46274 (J.A. Biegel); and a Fellowship from Alberta Cancer Board Translational Research in Cancer Program (Y.Wu).

References

1. Beckwith JB, Palmer NF. Histopathology and prognosis of Wilms tumors: results from the First National Wilms' Tumor Study. *Cancer* 1978;41:1937–1948. [PubMed: 206343]
2. Rorke LB, Packer RJ, Biegel JA. Central nervous system atypical teratoid/rhabdoid tumors of infancy and childhood: definition of an entity. *J Neurosurg* 1996;85:56–65. [PubMed: 8683283]
3. Parham DM, Weeks DA, Beckwith JB. The clinicopathologic spectrum of putative extrarenal rhabdoid tumors. An analysis of 42 cases studied with immunohistochemistry or electron microscopy. *Am J Surg Pathol* 1994;18:1010–1029. [PubMed: 8092393]
4. Biggs PJ, Garen PD, Powers JM, Garvin AJ. Malignant rhabdoid tumor of the central nervous system. *Hum Pathol* 1987;18:332–337. [PubMed: 3030922]
5. Biegel JA. Molecular genetics of atypical teratoid/rhabdoid tumor. *Neurosurg Focus* 2006;20:E11. [PubMed: 16459991]
6. Biegel JA, Rorke LB, Packer RJ, Emanuel BS. Monosomy 22 in rhabdoid or atypical tumors of the brain. *J Neurosurg* 1990;73:710–714. [PubMed: 2213160]
7. Biegel JA, Tan L, Zhang F, et al. Alterations of the hSNF5/INI1 gene in central nervous system atypical teratoid/rhabdoid tumors and renal and extrarenal rhabdoid tumors. *Clin Cancer Res* 2002;8:3461–3467. [PubMed: 12429635]
8. Oruetxebarria I, Venturini F, Kekarainen T, et al. P16INK4a is required for hSNF5 chromatin remodeler-induced cellular senescence in malignant rhabdoid tumor cells. *J Biol Chem* 2004;279:3807–3816. [PubMed: 14604992]
9. Isakoff MS, Sansam CG, Tamayo P, et al. Inactivation of the Snf5 tumor suppressor stimulates cell cycle progression and cooperates with p53 loss in oncogenic transformation. *Proc Natl Acad Sci U S A* 2005;102:17745–17750. [PubMed: 16301525]
10. Roberts CW, Galusha SA, McMenamin ME, Fletcher CD, Orkin SH. Haploinsufficiency of Snf5 (integrase interactor 1) predisposes to malignant rhabdoid tumors in mice. *Proc Natl Acad Sci US A* 2000;97:13796–13800.
11. Parato KA, Senger D, Forsyth PA, Bell JC. Recent progress in the battle between oncolytic viruses and tumours. *Nat Rev Cancer* 2005;5:965–976. [PubMed: 16294217]
12. Cui K, Taylor P, Liu H, et al. The chromatin-remodeling BAF complex mediates cellular antiviral activities by promoter priming. *Mol Cell Biol* 2004;24:4476–4486. [PubMed: 15121865]
13. Yang WQ, Senger D, Muzik H, et al. Reovirus prolongs survival and reduces the frequency of spinal and leptomeningeal metastases from medulloblastoma. *Cancer Res* 2003;63:3162–3172. [PubMed: 12810644]
14. Ochiai H, Moore SA, Archer GE, et al. Treatment of intracerebral neoplasia and neoplastic meningitis with regional delivery of oncolytic recombinant poliovirus. *Clin Cancer Res* 2004;10:4831–4838. [PubMed: 15269159]
15. Lun X, Yang W, Alain T, et al. Myxoma virus is a novel oncolytic virus with significant antitumor activity against experimental human gliomas. *Cancer Res* 2005;65:9982–9990. [PubMed: 16267023]
16. Jiang H, Conrad C, Fueyo J, Gomez-Manzano C, Liu TJ. Oncolytic adenoviruses for malignant glioma therapy. *Front Biosci* 2003;8:d577–d588. [PubMed: 12700119]
17. Connor JH, Naczki C, Koumenis C, Lyles DS. Replication and cytopathic effect of oncolytic vesicular stomatitis virus in hypoxic tumor cells in vitro and in vivo. *J Virol* 2004;78:8960–8970. [PubMed: 15308693]
18. Porosnicu M, Mian A, Barber GN. The oncolytic effect of recombinant vesicular stomatitis virus is enhanced by expression of the fusion cytosine deaminase/uracil phosphoribosyltransferase suicide gene. *Cancer Res* 2003;63:8366–8376. [PubMed: 14678998]
19. Lun X, Senger DL, Alain T, et al. Effects of i.v. administered recombinant vesicular stomatitis virus (VSV(ΔM51)) on multifocal and invasive gliomas. *J Natl Cancer Inst* 2006;98:1546–1557. [PubMed: 17077357]

20. Markert JM, Medlock MD, Rabkin SD, et al. Conditionally replicating herpes simplex virus mutant, G207 for the treatment of malignant glioma: results of a phase I trial. *Gene Ther* 2000;7:867–874. [PubMed: 10845725]
21. Freeman AI, Zakay-Rones Z, Gomori JM, et al. Phase I/II trial of intravenous NDV-HUJ oncolytic virus in recurrent glioblastoma multiforme. *Mol Ther* 2006;13:221–228. [PubMed: 16257582]
22. Shinozaki K, Ebert O, Kourmioti C, Tai YS, Woo SL. Oncolysis of multifocal hepatocellular carcinoma in the rat liver by hepatic artery infusion of vesicular stomatitis virus. *Mol Ther* 2004;9:368–376. [PubMed: 15006603]
23. Kerr P, McFadden G. Immune responses to myxoma virus. *Viral Immunol* 2002;15:229–246. [PubMed: 12081009]
24. Shisler JL, Moss B. Immunology 102 at poxvirus U: avoiding apoptosis. *Semin Immunol* 2001;13:67–72. [PubMed: 11289801]
25. Fenner, F.; Ross, J. Myxomatosis. In: Thompson, G.; King, C., editors. *The European rabbit, the history and biology of a successful colonizer*. Oxford: Oxford University Press; 1994. p. 205-239.
26. Burnet, F. *Changing patterns: an atypical autobiography*. Melbourne (Australia): W. Heinemann; 1968. p. 105-120.
27. Sypula J, Wang F, Ma Y, Bell J, McFadden G. Myxoma virus tropism in human tumor cells. *Gene Ther Mol Biol* 2004;8:103–114.
28. Stanford MM, Barrett JW, Nazarian SH, Werden S, McFadden G. Oncolytic virotherapy synergism with signaling inhibitors: Rapamycin increases myxoma virus tropism for human tumor cells. *J Virol* 2007;81:1251–1260. [PubMed: 17108021]
29. Barber GN. VSV-tumor selective replication and protein translation. *Oncogene* 2005;24:7710–7719. [PubMed: 16299531]
30. Stojdl DF, Lichty BD, tenOever BR, et al. VSV strains with defects in their ability to shutdown innate immunity are potent systemic anti-cancer agents. *Cancer Cell* 2003;4:263–275. [PubMed: 14585354]
31. Stojdl DF, Lichty B, Knowles S, et al. Exploiting tumor-specific defects in the interferon pathway with a previously unknown oncolytic virus. *Nat Med* 2000;6:821–825. [PubMed: 10888934]
32. Ebert O, Shinozaki K, Huang TG, et al. Oncolytic vesicular stomatitis virus for treatment of orthotopic hepatocellular carcinoma in immune-competent rats. *Cancer Res* 2003;63:3605–3611. [PubMed: 12839948]
33. Ebert O, Harbaran S, Shinozaki K, Woo SL. Systemic therapy of experimental breast cancer metastases by mutant vesicular stomatitis virus in immunocompetent mice. *Cancer Gene Ther* 2005;12:350–358. [PubMed: 15565179]
34. Shinozaki K, Ebert O, Woo SL. Treatment of multifocal colorectal carcinoma metastatic to the liver of immune-competent and syngeneic rats by hepatic artery infusion of oncolytic vesicular stomatitis virus. *Int J Cancer* 2005;114:659–664. [PubMed: 15609320]
35. Balachandran S, Barber GN. Vesicular stomatitis virus (VSV) therapy of tumors. *IUBMB Life* 2000;50:135–138. [PubMed: 11185959]
36. Ota S, Crabbe DC, Tran TN, Triche TJ, Shimada H. A study with two established cell lines. Malignant rhabdoid tumor. *Cancer* 1993;71:2862–2872. [PubMed: 8385567]
37. Karnes PS, Tran TN, Cui MY, et al. Establishment of a rhabdoid tumor cell line with a specific chromosomal abnormality, 46,XY t(11;22)(p15.5;q11.23). *Cancer Genet Cytogenet* 1991;56:31–38. [PubMed: 1747867]
38. Johnston JB, Barrett JW, Chang W, et al. Role of the serine-threonine kinase PAK-1 in myxoma virus replication. *J Virol* 2003;77:5877–5888. [PubMed: 12719581]
39. Burger PC, Yu IT, Tihan T, et al. Atypical teratoid/rhabdoid tumor of the central nervous system: a highly malignant tumor of infancy and childhood frequently mistaken for medulloblastoma: a Pediatric Oncology Group study. *Am J Surg Pathol* 1998;22:1083–1092. [PubMed: 9737241]
40. Packer RJ, Biegel JA, Blaney S, et al. Atypical teratoid/rhabdoid tumor of the central nervous system: report on workshop. *J Pediatr Hematol Oncol* 2002;24:337–342. [PubMed: 12142780]
41. Wang G, Barrett JW, Stanford M, et al. Infection of human cancer cells with myxoma virus requires Akt activation via interaction with a viral ankyrin-repeat host range factor. *Proc Natl Acad Sci U S A* 2006;103:4640–4645. [PubMed: 16537421]

42. Charboneau A, Chai J, Jordan J, et al. P-Akt expression distinguishes two types of malignant rhabdoid tumors. *J Cell Physiol* 2006;209:422–427. [PubMed: 16897758]
43. Wollmann G, Tattersall P, van den Pol AN. Targeting human glioblastoma cells: comparison of nine viruses with oncolytic potential. *J Virol* 2005;79:6005–6022. [PubMed: 15857987]
44. Lang FF, Bruner JM, Fuller GN, et al. Phase I trial of adenovirus-mediated p53 gene therapy for recurrent glioma: biological and clinical results. *J Clin Oncol* 2003;21:2508–2518. [PubMed: 12839017]
45. Bell JC, Lichty B, Stojdl D. Getting oncolytic virus therapies off the ground. *Cancer Cell* 2003;4:7–11. [PubMed: 12892708]
46. Power AT, Wang J, Falls TJ, et al. Carrier cell-based delivery of an oncolytic virus circumvents antiviral immunity. *Mol Ther* 2007;15:123–130. [PubMed: 17164783]
47. Lun XQ, Zhou H, Alain T, et al. Targeting human medulloblastoma: oncolytic virotherapy with myxoma virus is enhanced by rapamycin. *Cancer Res* 2007;67:8818–8827. [PubMed: 17875723]

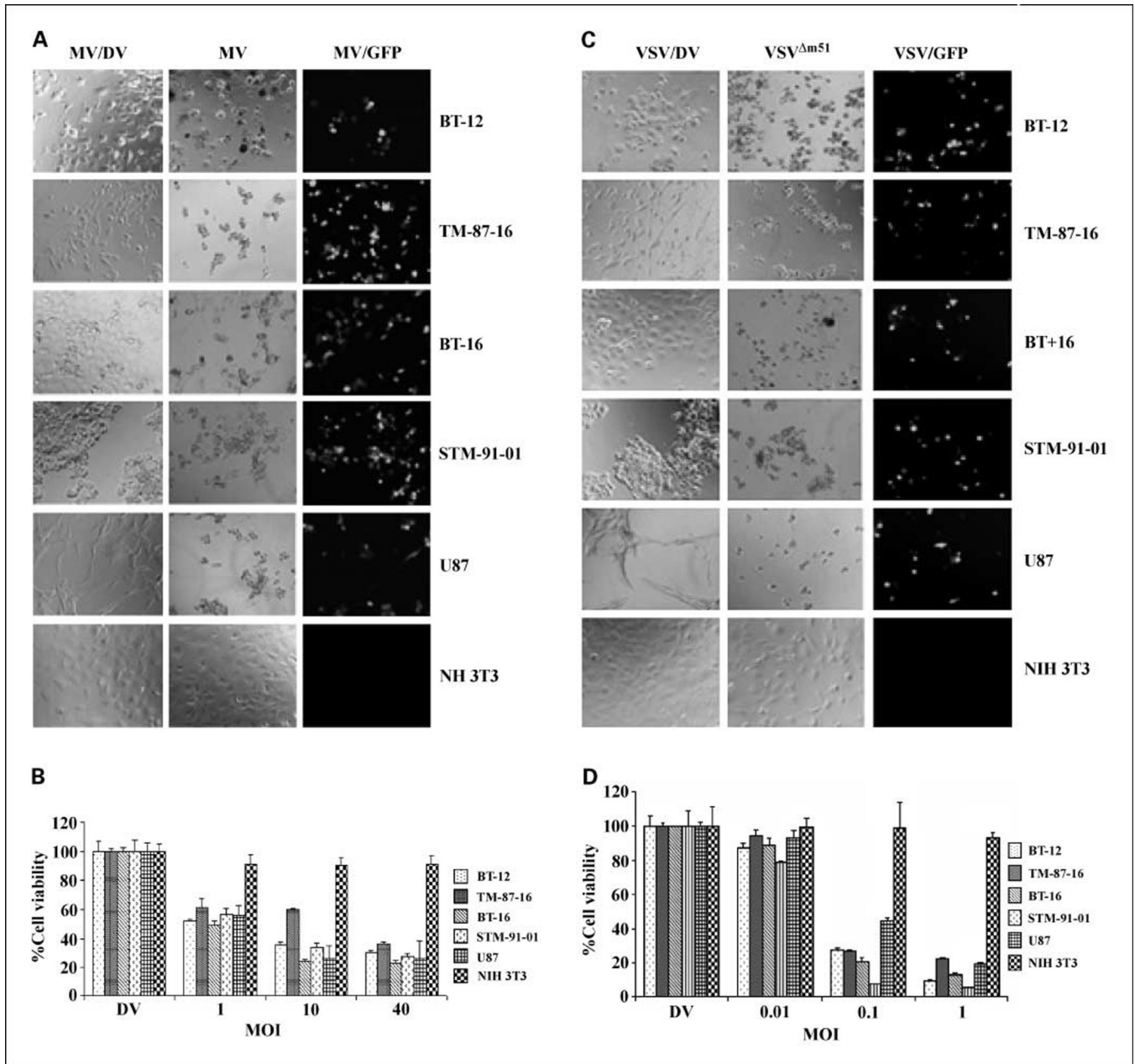


Fig. 1. Rhabdoid tumor cell lines are susceptible to oncolysis by MV and VSV Δ M51 *in vitro*. *A*, rhabdoid tumor cell lines were infected with 10 MOI of live MV or UV-inactivated dead MV (MV/DV). CPE (*middle column*) and expression of virally encoded GFP (*right column*) were evident in all malignant rhabdoid tumor cell lines 72 h after exposure to live MV (magnification, $\times 200$). *B*, relative cell viability was measured using MTT assays 72 h postinfection with the indicated MOI of MV. *C*, tumor cell lines were infected with 1 MOI of live or UV-inactivated dead VSV Δ M51 (VSV/DV). CPE (*middle column*) and expression of virally encoded GFP (*right column*) were evident in all rhabdoid tumor cell lines 72 h after exposure to live VSV Δ M51 (magnification, $\times 200$). *D*, relative cell viability was measured using MTT assays 72 h postinfection with the indicated MOI of VSV Δ M51. U87 glioma cells and NIH 3T3 cells served as positive and negative controls, respectively.

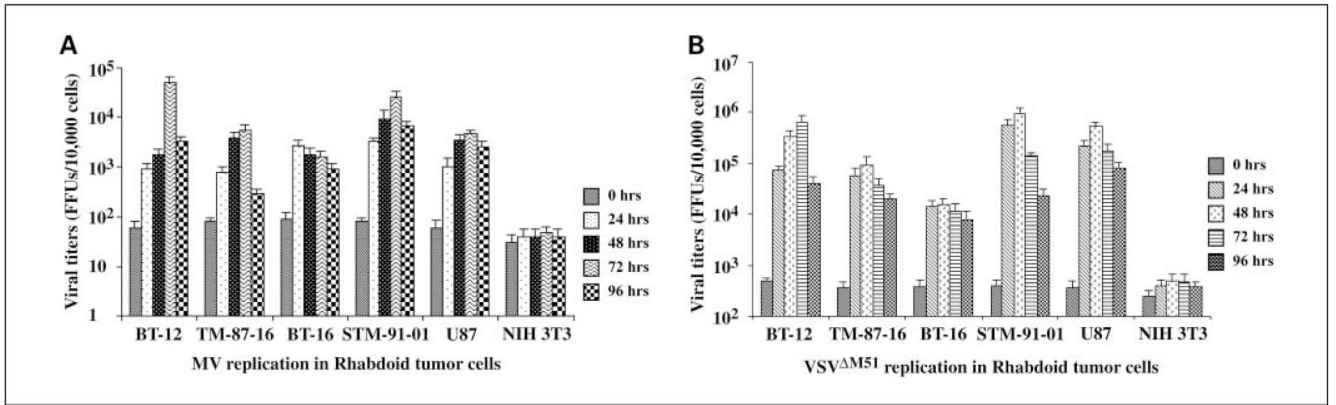


Fig. 2.

Oncolytic viruses replicate in rhabdoid tumor cell lines *in vitro*. Rhabdoid tumor cell lines were infected with 0.1 MOI of MV or VSV $\Delta M51$. Viral titers of (A) MV or (B) VSV $\Delta M51$ in rhabdoid tumor cells were determined using a standard focus or plaque formation assay on BGMK or L929 cell lines, respectively. Green fluorescent foci were viewed and counted under the fluorescent microscope, and viral titers were based on 10,000 cells. Titers of MV and VSV $\Delta M51$ increased in all four rhabdoid tumor cell lines by 24 h postinfection, and remained elevated over original input doses up to 96 h postinfection. U87 glioma cells and NIH 3T3 cells served as positive and negative controls, respectively.

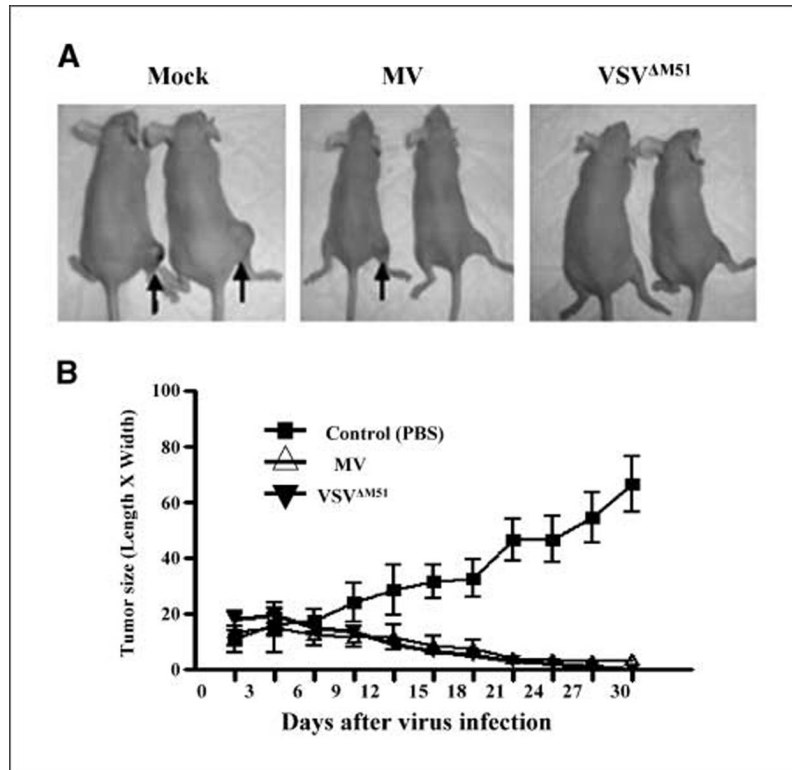


Fig. 3. I.t. injection of MV and VSV Δ M51 reduced the size of s.c. malignant rhabdoid tumor in CD-1 nude mice. Mice bearing STM-91-01 (5×10^5 cells per mouse) s.c. tumors in their hind flank were injected i.t. with MV or VSV Δ M51 (1×10^7 pfu/mouse/injection, three injections at 2 d intervals) or PBS as a control (four mice in each treatment group). **A**, representative photographs of the effect of various treatments on mice implanted with s.c. malignant rhabdoid tumor xenografts. Black arrows, s.c. tumors. Large tumors were present in control mice injected with PBS (mock), whereas no tumor or only small residual tumors were present after treatment with MV and VSV Δ M51. **B**, tumor sizes in each group were measured and compared (Δ , MV; \blacktriangledown , VSV Δ M51; \blacksquare , PBS). Points, mean of the tumor size; bars, 95% confidence interval.

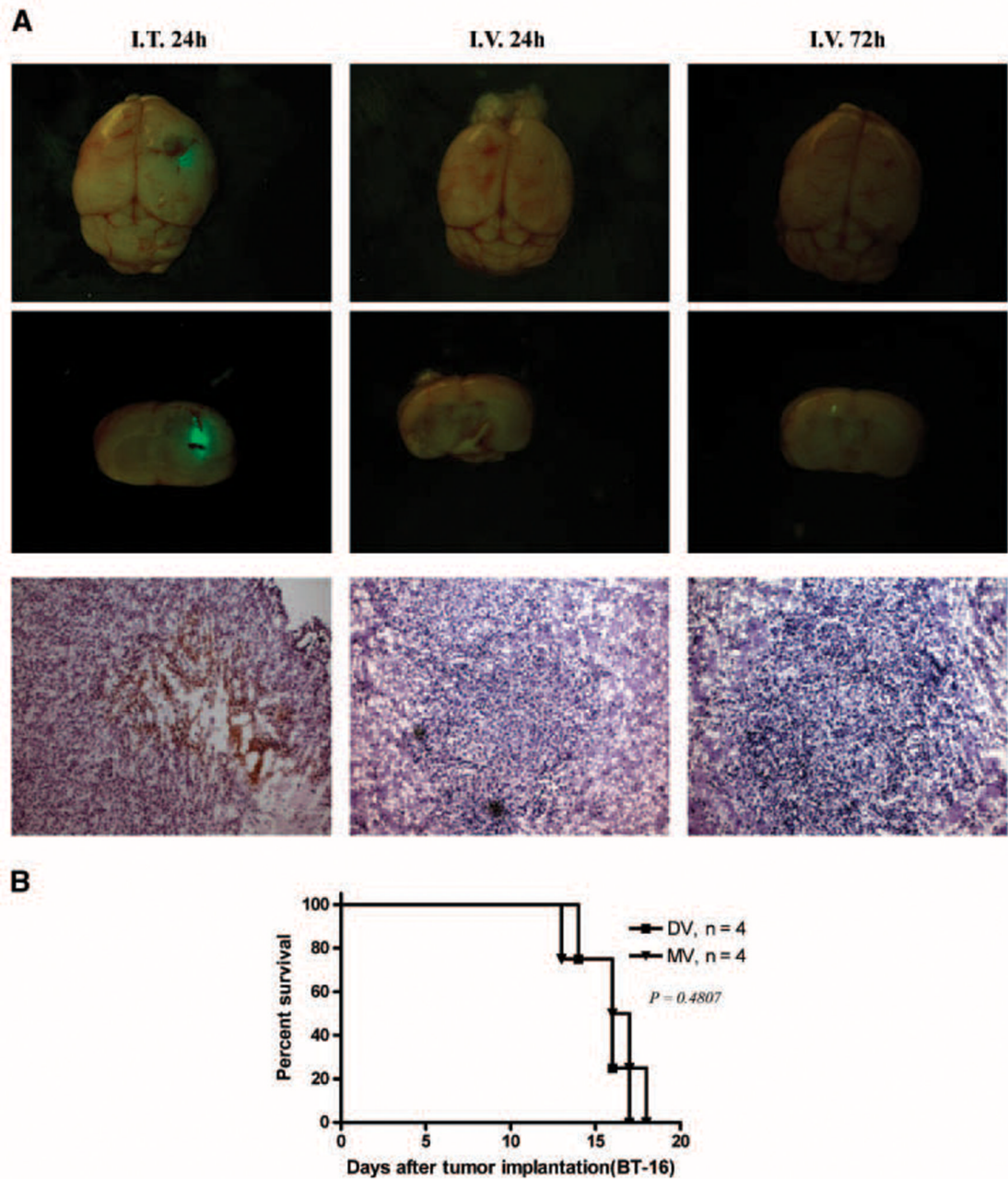
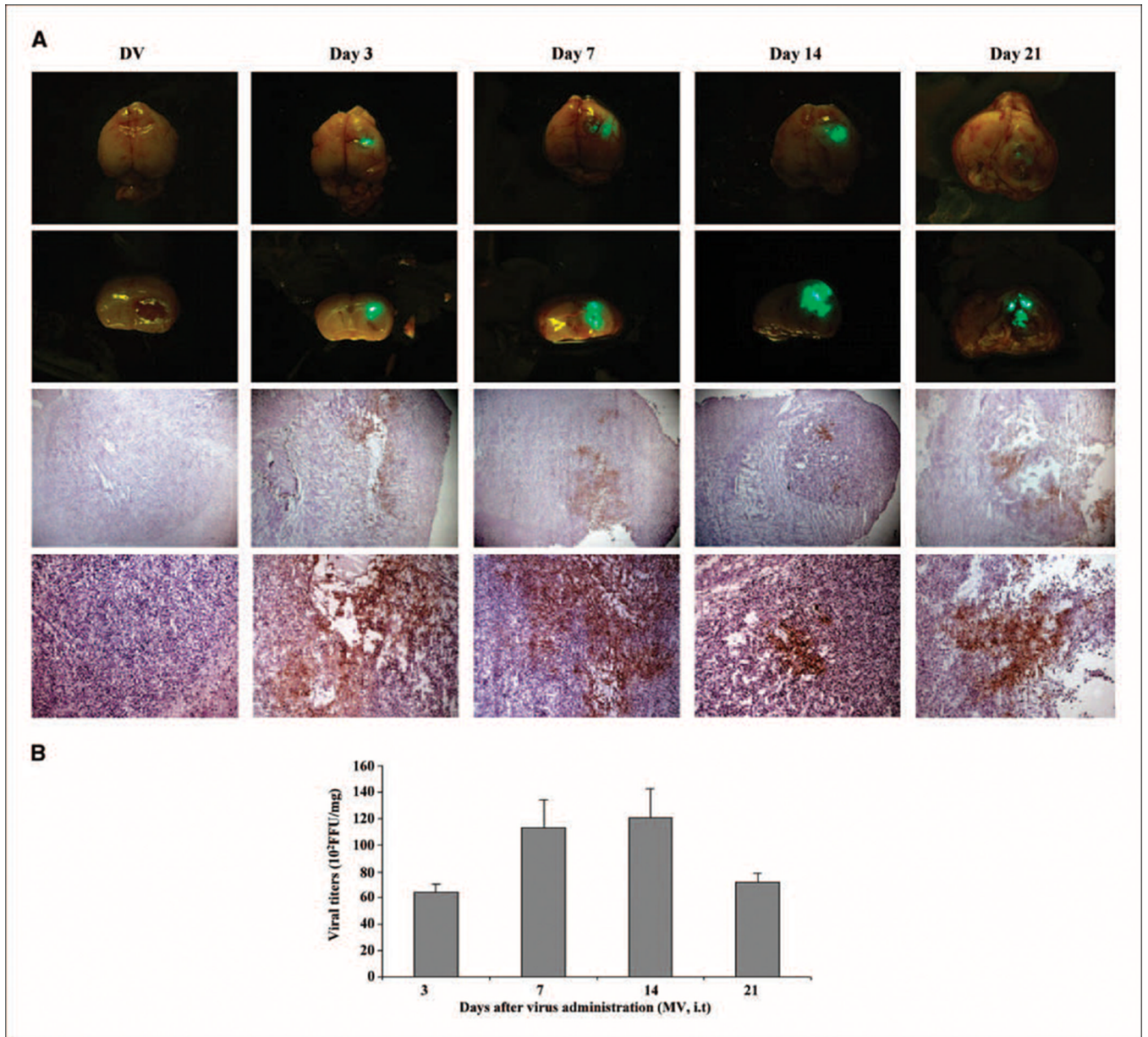


Fig. 4. Distribution and survival of i.v. administered MV in nude mice bearing BT-16 rhabdoid tumors. *A*, nude mice bearing BT-16 intracranial tumors were treated with MV (i.v.) at a dose of 5×10^7 pfu/mouse (the highest dose of virus available) 10 d after tumor cell implantation. Animals were sacrificed at different time points (24 h, 72 h) after virus infection. Top and middle lane, photomicrograph of GFP-labeled virus present in the rhabdoid tumor ($n = 3$ mice per group; magnification, $\times 20$). Arrows, GFP virus expression. Bottom row, immunohistochemical staining for MT-7 protein (arrow, brown staining; magnification, $\times 100$). Left column, MV i.t. (5×10^6 pfu/mice) as a positive control. *B*, Kaplan-Meier showing the survival of BT-16 tumor-

bearing mice after i.v. administration of PBS (DV, $n = 4$; MV, $n = 4$). All P values are two-sided. I.v. delivery of MV did not prolong survival (DV and MV, log-rank test, $P = 0.4807$).



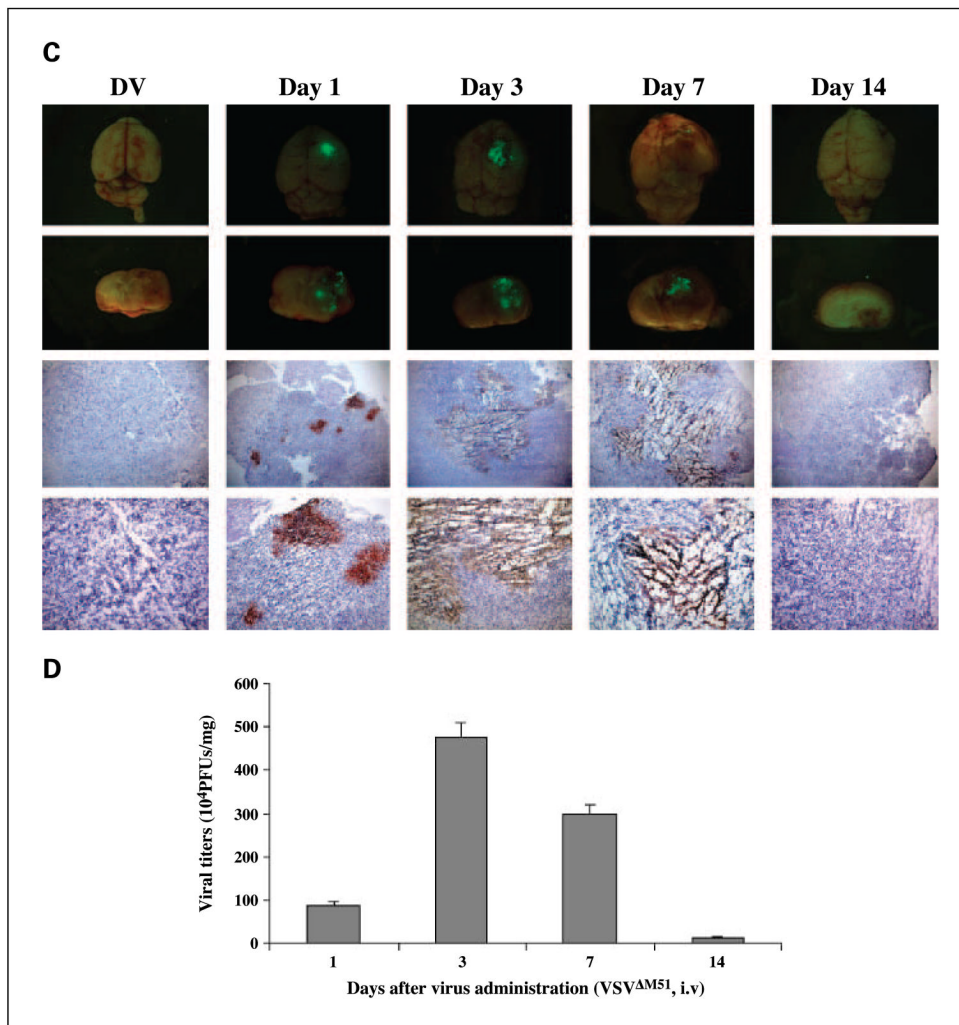


Fig. 5. *In vivo* distribution of MV and VSV Δ M51 in CD-1 nude mice bearing atypical teratoid/rhabdoid tumor brain xenografts. MV (A) and VSV Δ M51 (C) viral GFP expression were observed *in vivo* using immunofluorescence microscopy (*first* and *second* row). Immunohistochemical staining of MV and VSV Δ M51 proteins on consecutive brain sections (*bottom two rows*) confirms the presence of viral proteins in the rhabdoid tumor cells (*brown staining*; magnification, *top to bottom*, $\times 25$, $\times 100$). Viral recovery assays done with tumor tissue confirmed the presence of infectious, replication-competent MV (B) and VSV Δ M51 (D) *in vivo* at various time points after injection of viruses. Control tumors were injected with UV-inactivated (DV) MV (A) or UV-inactivated (DV) VSV Δ M51 (C).

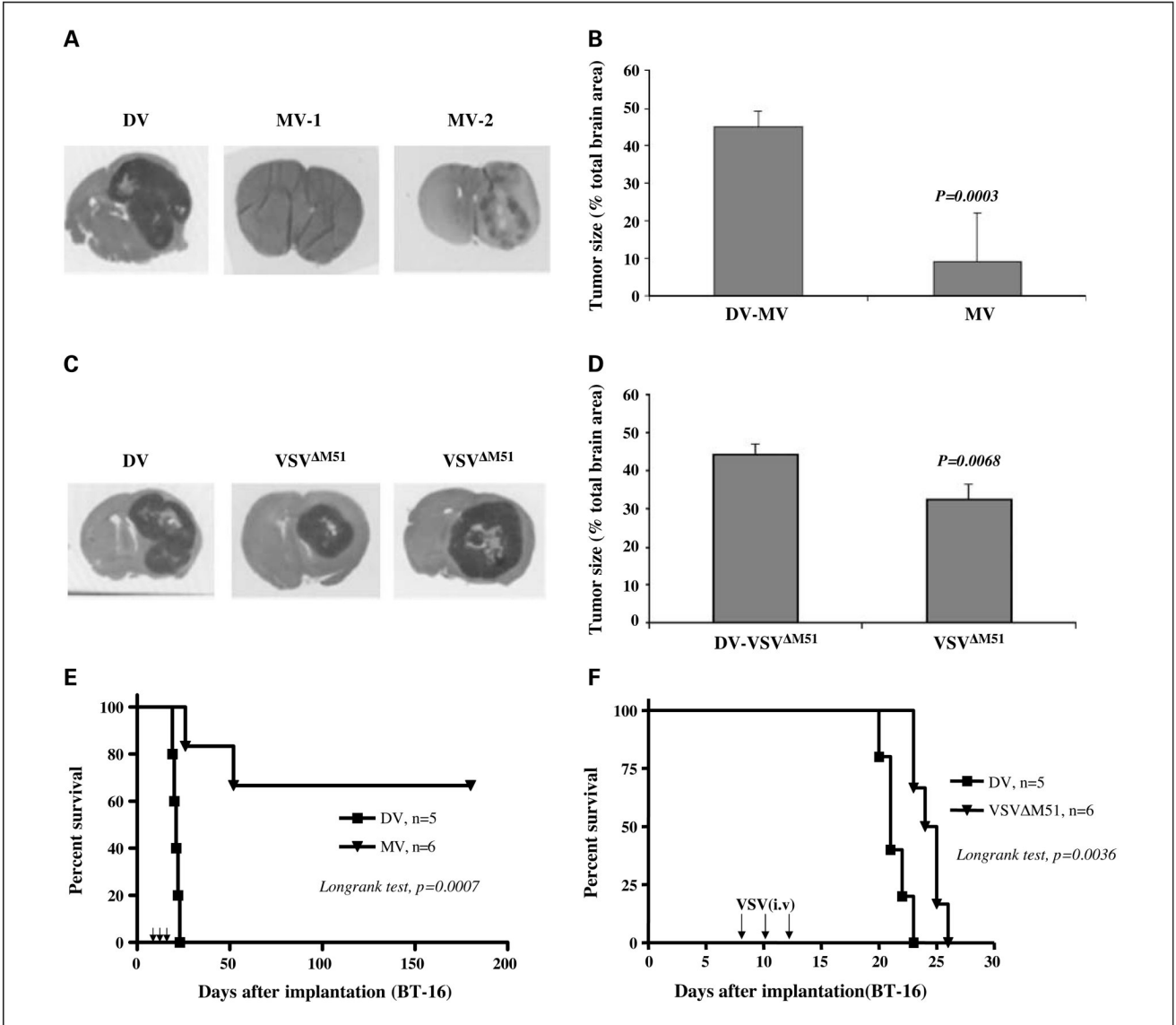


Fig. 6.

MV and VSV Δ M51 decrease tumor size and prolongs survival of CD-1 nude mice bearing atypical teratoid/rhabdoid tumor brain xenografts. BT-16 cells were implanted in the brains of nude mice (2×10^5 cells per mouse) on day 0. Live or UV-inactivated (DV) MV (1×10^7 pfu/mouse/injection, i.t.) or VSV Δ M51 (5×10^8 pfu/mouse/injection, i.v.) were injected on days 8, 10, and 12. Treatment with MV (A and B) or VSV Δ M51 (C and D) significantly reduced the size of atypical teratoid/rhabdoid tumor brain xenografts 25 d after tumor implantation. Bars, 95% confidence intervals. E, the median survival of MV-treated mice ($n = 6$) was significantly longer than that of DV controls ($n = 5$, log-rank, $P = 0.0007$). F, VSV Δ M51 – treated (F) mice ($n = 6$) also survived longer than DV controls ($n = 5$, log-rank, $P = 0.0036$).